USCAP

ARTICLE

Defining the spatial landscape of *KRAS* mutated congenital pulmonary airway malformations: a distinct entity with a spectrum of histopathologic features

Nya D. Nelson[1,2], Feng Xu[1], Prashant Chandrasekaran[3], Leslie A. Litzky[2], William H. Peranteau[4], David B. Frank[3], Marilyn Li[1] and Jennifer Pogoriler[1]✉

The potential pathogenetic mechanisms underlying the varied morphology of congenital pulmonary airway malformations (CPAMs) have not been molecularly determined, but a subset have been shown to contain clusters of mucinous cells (MCC). These clusters are believed to serve as precursors for potential invasive mucinous adenocarcinoma, and they are associated with *KRAS* codon 12 mutations. To assess the universality of *KRAS* mutations in MCCs, we sequenced exon 2 of *KRAS* in 61 MCCs from 18 patients, and we found a *KRAS* codon 12 mutation in all 61 MCCs. Furthermore, all MCCs from a single patient always had the same *KRAS* mutation, and the same *KRAS* mutation was also found in non-mucinous lesional tissue. Next generation sequencing of seven MCCs showed no other mutations or copy number variations. Sequencing of 46 additional CPAMs with MCCs revealed *KRAS* mutations in non-mucinous lesional tissue in all cases. RNA in situ hybridization confirmed widespread distribution of cells with mutant *KRAS* RNA, even extending outside of the bronchiolar type epithelium. We identified 25 additional CPAMs with overall histologic architecture similar to CPAMs with *KRAS* mutations but without identifiable MCCs, and we found *KRAS* mutations in 17 (68%). The histologic features of these *KRAS* mutated CPAMs included type 1 and type 3 morphology, as well as lesions with an intermediate histologic appearance, and analysis revealed a strong correlation between the specific amino acid substitution and histomorphology. These findings, together with previously published model organism data, suggests that the formation of type 1 and 3 CPAMs is driven by mosaic *KRAS* mutations arising in the lung epithelium early in development and places them within the growing field of mosaic RASopathies. The presence of widespread epithelial mutation explains late metastatic disease in incompletely resected patients and reinforces the recommendation for complete resection of these lesions.

Modern Pathology (2022) 35:1870–1881; https://doi.org/10.1038/s41379-022-01129-0

INTRODUCTIONS

Congenital pulmonary airway malformations (CPAMs) comprise a spectrum of cystic and non-cystic lung malformations. Multiple classification schemes utilizing a combination of gross and histologic features have been proposed for these lesions[1–4], the most widely adopted of which is the Stocker classification. This system proposed that each morphologic type represented lesions arising at different levels of the lung from trachea to alveoli; however, over time our understanding of the pathogenesis, clinical significance, and histologic classification of these lesions has evolved. Notably, lesions that were once classified as Stocker type 4 CPAMs[2] are now known to represent cystic pleuropulmonary blastomas[5], with an underlying heterozygous germline *DICER1* mutation in 66% of patients[6]. Similarly, Stocker type 0 CPAMs are now recognized as a diffuse developmental lung anomaly termed acinar dysplasia, and are associated with *TBX4*, *FGF10* and *FGFR2* mutations[7,8].

Genetic associations for the remaining Stocker types 1-3 are not known, but the idea of a bronchial atresia sequence in which airway obstruction during development leads to parenchymal maldevelopment is well established in pediatric pathology[3,9,10]. It has been hypothesized that the location, degree, or timing of obstruction could relate to variable morphology. However, the specific morphology of the CPAMs in most of these series is either not documented or is consistent with type 2. Evidence associating CPAMs type 1 and 3 with bronchial atresia is limited.

The underlying cause and any potential genetic associations in type 1 and 3 CPAMs therefore remains elusive. Studies examining mucinous cell clusters (MCCs), which are found predominantly in type 1 CPAMs[11], may provide some insight into potential genetic associations. Several small studies have described *KRAS* codon 12 mutations in MCCs, and this has led many to hypothesize that MCCs may serve as a precursor lesion for metastatic mucinous adenocarcinoma in patients with unresected type 1 CPAMs[12–14]. However, the evidence for *KRAS* mutations in MCCs is conflicting, with one study reporting *KRAS* mutations in only a subset of MCCs[12] and conflicting reports as to whether distinct MCCs within

[1]Department of Pathology and Laboratory Medicine, The Children's Hospital of Philadelphia, Perelman School of Medicine at the University of Pennsylvania, Philadelphia, PA, USA. [2]Department of Pathology and Laboratory Medicine, Hospital of the University of Pennsylvania, Perelman School of Medicine at the University of Pennsylvania, Philadelphia, PA, USA. [3]Department of Pediatrics, The Children's Hospital of Philadelphia, Perelman School of Medicine at the University of Pennsylvania, Philadelphia, PA, USA. [4]Department of Surgery, The Children's Hospital of Philadelphia, Perelman School of Medicine at the University of Pennsylvania, Philadelphia, PA, USA. ✉email: pogorilerj@chop.edu

Received: 7 March 2022 Revised: 9 June 2022 Accepted: 10 June 2022
Published online: 6 July 2022

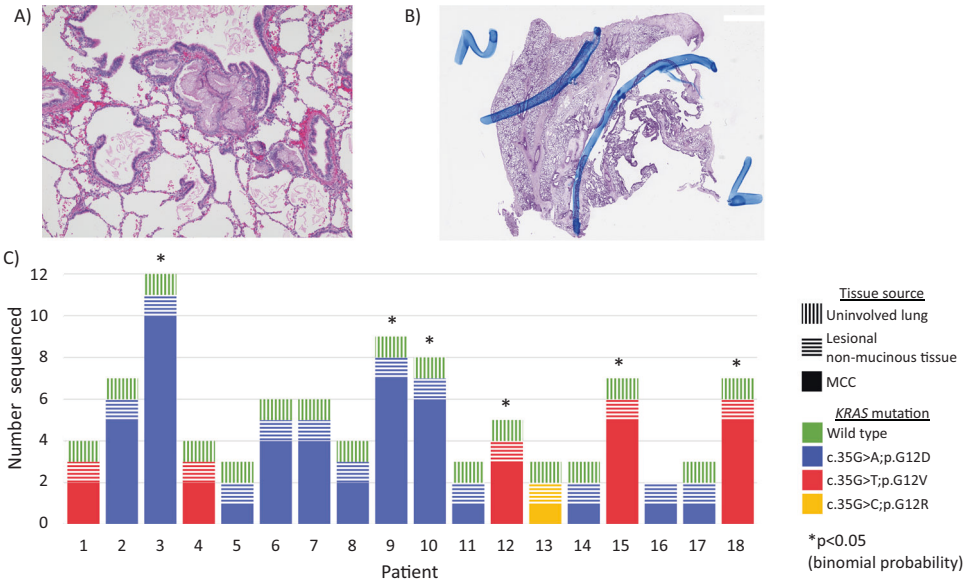

Fig. 1 Congenital pulmonary airway malformations with mucinous cell clusters (MCCs) contain *KRAS* codon 12 mutations within MCCs and throughout the lesion. MCCs from separate blocks (**A**), lesional tissue without MCCs (**B**), and normal lung tissue (**B**) were macrodissected from 20 µm thick FFPE tissue sections. **C** Within each patient, the same *KRAS* codon 12 mutation was found throughout the lesion, including in each MCC. Adjacent uninvolved lung always had wild type *KRAS* sequence. *$p < 0.05$, binomial distribution.

a single lesion have the same or different *KRAS* mutations[12–14]. Additionally, a recent small series identified *KRAS* mutations not only in MCCs, but also in non-mucinous lesional tissue in a subset of CPAMs, including those with no histologically identifiable MCCs[15]. These studies raise multiple questions regarding the universality, or lack thereof, of *KRAS* mutations in MCCs and non-mucinous CPAM epithelium, and whether *KRAS* mutations are in fact a universal feature of a subset of CPAMs.

Large scale studies have described MCCs as a common feature in up to 83% of type 1 CPAMs[1,11]. Additionally, they have been rarely described in type 2[15,16] and type 3 CPAMs[16,17], calling into question whether MCCs can truly occur in any CPAM regardless of histologic classification, or if there are perhaps distinct and reproducible histologic criteria that unite CPAMs with MCCs. Further complicating this, the existence of type 3 CPAMs as a distinct entity has been controversial, with some noting the histologic resemblance to pulmonary hyperplasia in the setting of laryngeal atresia and suggesting that they may be best considered a localized form of pulmonary hyperplasia[3].

We sought to better characterize the *KRAS* mutational landscape in MCCs and non-mucinous CPAM tissue in a large cohort of CPAMs, and to combine this with histologic data in order to identify morphologic features that can reliably identify *KRAS* mutated CPAMs.

MATERIALS AND METHODS

Case identification

With institutional review board approval (eIRB 20-017451), CPAMs were identified via a database search of surgical pathology reports issued by the Children's Hospital of Philadelphia between January 2000 and March 2020. Cases were reviewed to identify CPAMs with MCCs for inclusion within this study. Additional cases with similar histologic features as CPAMs with MCCs were also identified. Those features include classic type 1 morphology, classic type 3 morphology, and lesions with overlapping histologic features that were characterized as type 1/3 CPAMs (see results for detailed histologic features of these lesions). Cases of intrapulmonary bronchogenic cysts, classic type 2 CPAMs, bronchial atresia, and intra- and extra-lobar sequestrations were excluded. Clinical information was obtained via retrospective chart review.

Adult mucinous adenocarcinomas were identified via a database search of surgical pathology reports issued by the Hospital of the University of Pennsylvania during the same time period. Mucinous adenocarcinomas were reviewed to identify those with predominantly lepidic architecture for use as controls.

Macrodissection

Each case with MCCs was evaluated for clusters of sufficient size for macrodissection (Fig. 1A), and each MCC was dissected from a different block to ensure that they were separate foci. Whenever possible, non-mucinous lesional tissue was dissected from a block that lacked MCCs. When MCCs were present in all blocks, non-mucinous tissue was macrodissected from an area as far as possible from the MCCs. Additionally, when possible, normal lung was macrodissected from the same block used for lesional sequencing (Fig. 1B). For cases without MCCs, lesional tissue and normal lung tissue were macrodissected from the same block when possible.

Dissection of lesional tissue focused on areas that were predominantly lined by columnar epithelium. For each formalin fixed paraffin embedded (FFPE) tissue block with tissue of interest, multiple 20 µm unstained sections were cut with flanking periodic acid-Schiff (PAS) stained slides to aid in identification of the region of interest and highlight any MCCs present. Given the distinct cell shape, even small clusters of mucinous cells could be confirmed and their precise location marked on the unstained slides prior to macrodissection. To ensure that there was no cross contamination, each area of interest was macrodissected using a fresh scalpel blade.

DNA extraction, PCR amplification, and Sanger Sequencing

DNA was isolated using the laboratory standard protocol and amplified using primers specifically designed to cover exon 2 of the *KRAS* gene (NM_004985.5) and to detect mosaic mutations with a variant allele frequency (VAF) of ≥5%. Polymerase chain reaction (PCR) was performed following the laboratory standard procedure. PCR products were then cleaned, and Sanger sequenced according to the laboratory standard procedures. Sequencing data were analyzed by comparing to the reference sequence using Mutation Surveyor (SoftGenetics, PA).

Next generation sequencing

Next generation sequencing (NGS) was performed using the CHOP Comprehensive Solid Tumor Panel (CSTP). The panel interrogates 238 genes associated with adult and pediatric solid tumors and covers all coding exons and at least 10 bp of flanking intronic sequences, certain promoter regions, and known pathogenic intronic variants[18]. An additional 1038 common single nucleotide polymorphisms (SNPs) were added to the

panel to mimic a low-density SNP array to facilitate the identification of copy number variations (CNVs). NGS libraries were constructed using 50 ng of genomic DNA and SureSelect QXT reagent kit (Agilent Technologies, Santa Clara, CA). Libraries were sequenced using Illumina Hiseq 2500 with 150 bp pair-end reads (Illumina, San Diego, CA). Sequence data were analyzed using an in-house bioinformatics pipeline for sequence variant detection and NextGene (SoftGenetics, PA) for CNV evaluation[18]. All variants identified by the pipeline were carefully reviewed and visualized using Integrative Genomics Viewer (IGV)[19] when necessary.

Fluorescence in situ hybridization (FISH)

FISH was performed by the Hospital of the University of Pennsylvania Cytogenetics Laboratory. FFPE tissue was analyzed using Dual Color Deletion probes for *EGR1*(5q31)/5p15.2 (XL Del(5)(q31) (MetaSystems USA) or D7S486 (7q31)/7p11-q11 (CL 7q31 (D7S486) (MetaSystems USA) under standard hybridization conditions.

Histologic characterization

Hematoxylin and eosin-stained slides were reviewed and characterized by two pathologists (N.D.N. and J.P.) blinded to the results of *KRAS* exon 2 sequencing. For cases with MCCs, the total number of MCCs, blocks with MCCs, and total lesional blocks were recorded.

Each lesion was assessed for complexity and for the most consistent histologic category using the Stocker classification[2]. Lesions with true papillary projections, branching papillae, or irregular small cysts were categorized as complex. Sawtooth appearance of large cyst lining was not considered sufficient to characterize a case as complex in appearance. Lesions were categorized as type 1, type 3, or a hybrid lesion with features of both type 1 and 3 (type 1/3). Therapy related changes, including thoracoamniotic shunt related squamous metaplasia, were ignored in the histologic analysis.

BaseScope™ RNA in situ hybridization (ISH)

BaseScope™ RNA ISH (Advanced Cell diagnostics, Newark, CA) allows the detection of short RNA targets including point mutations in RNA transcripts. Previously validated *KRAS* wild type (WT) and *KRAS* c.35 G > A (G12D) mutant 1ZZ probes were used to characterize the spatial landscape of WT and mutant alelles[20]. The *dapB* probe and *POLR2A* probes were used for the negative and positive controls for each FFPE tissue sample studied, respectively. Target retrieval, binding, and amplification of signal was performed according to the established BaseScope™ protocol. In brief, sections were baked at 60 °C for 1 hour, deparaffinized with xylene (2 × 5 minutes) and ethanol (2 × 2 minutes), dried again at 60 °C for 15 minutes, to avoid section delamination. Sections were then incubated with hydrogen peroxide for 10 minutes, rinsed in distilled water and, were finally treated with target retrieval for 15 minutes at 99–102 °C. Sections were then rinsed twice with distilled water, and dried again at 60 °C for 15 minutes. These sections were then pretreated with protease III for 20 minutes at 40 °C and then rinsed twice with distilled water. The BaseScope™ probes were then hybridized for 2 hours at 40 °C in HybEZ oven before further incubation with reagents Amp1 (30 minutes), Amp2 (30 minutes), Amp3 (15 minutes), Amp4 (30 minutes), Amp5 (30 minutes) and Amp6 (15 minutes) at 40 °C in HybEZ oven. The sections were finally incubated with Amp7 (30 minutes) and Amp8 (15 minutes) at RT. These sections were washed with wash buffer (2 × 2 minutes) between each Amp step. Sections were finally stained with Fast Red for 10 minutes at RT and counterstained with Gill's hematoxylin before finally drying at 60 °C and mounted with VectaMount permanent mounting medium (Vector Labs, Burlingame, CA).

Statistics

Statistical analyses were conducted using Rstudio[21] and the tidyverse[22] and rstatix[23] libraries.

RESULTS

Mucinous cell cluster sequencing

Sixty-four CPAMs with MCCs were identified in resections spanning a 20-year period. Each case was evaluated for MCCs of sufficient size for macrodissection (Fig. 1A). In total, *KRAS* sequencing was performed on 61 MCCs from 18 patients, with a median of 2.5 clusters sequenced per patient and up to 10 clusters (each from a separate block) sequenced in a single patient. The histologic features of MCCs in 44 of these patients were reported previously[17], and the size and extent of MCCs in the additional cases was subjectively similar. Only 2 patients were over one year of age, and the MCCs in those cases remained small (<1 mm). In no cases were mucinous cells seen outside of lesional tissue, and they did not form a mass lesion.

KRAS codon 12 mutations were identified in all 61 sequenced MCCs. *KRAS* p.G12D was the most common mutation and was detected in 70% ($n = 43$) of the MCCs and 67% ($n = 12$) of patients, followed by p.G12V in 28% ($n = 17$) of MCCs and 28% ($n = 5$) of patients. A *KRAS* p.G12R mutation was detected in one MCC. For each patient, the same *KRAS* mutation was identified in all sequenced MCCs (Fig. 1C). In six patients there were sufficient clusters for this distribution to be statistically significant based on overall mutation frequencies (Fig. 1C, $p < 0.05$, binomial distribution), while in the remaining 12 patients there were insufficient MCCs sequenced to determine statistical significance.

Next generation sequencing of MCCs

Adult pulmonary mucinous adenocarcinomas with *KRAS* mutations frequently harbor additional mutations and copy number variations[24–26]. To determine whether a similar genetic landscape is seen in MCCs, clusters with sufficient DNA quantity and quality were sequenced using the 238-gene NGS CSTP panel, and the results were compared to four adult minimally invasive mucinous adenocarcinomas. NGS results confirmed all *KRAS* mutations within MCCs and did not identify any additional clinically significant mutations or copy number variations (Supplementary Table 1). Macrodissected MCCs were estimated to contain approximately 15–40% mucinous cells (median 20% mucinous cells), and the *KRAS* VAF in these specimens was 20–33% (median 23%).

In contrast to MCCs, which universally had *KRAS* mutations, one adult mucinous adenocarcinoma had a wild type *KRAS* sequence. Additionally, two out of four adenocarcinomas had additional disease associated mutations, and two out of four had copy number variations that were confirmed using FISH (Supplementary Table 1).

KRAS sequencing of non-mucinous lesional CPAM tissue

A recent small study identified *KRAS* codon 12 mutations in both mucinous and non-mucinous but lesional CPAM tissue[15]. This, together with the higher-than-expected VAF seen with NGS and the identification of only a single mutation in each patient, led us to hypothesize that non-mucinous areas of the CPAMs in our study could also harbor *KRAS* codon 12 mutations. To address this, we first sequenced non-mucinous lesional CPAM tissue from the original 18 specimens (Fig. 1B). We identified *KRAS* codon 12 mutations in all 18 patients (Fig. 1C). In each patient, the same *KRAS* mutation was found within MCCs and the non-mucinous lesional tissue. In contrast, sequencing of normal adjacent lung from the 17 patients with sufficient normal tissue revealed a wild type *KRAS* exon 2 sequence in all patients (Fig. 1C).

We next expanded the study to include 46 additional CPAMs with MCCs, for a total of 64 CPAMs with MCCs. All 46 additional CPAMs harbored *KRAS* exon 2 mutations in the non-mucinous lesional tissue. In one patient with a grossly solid lesion that was histologically composed of multiple small foci, an initial sample using tissue from a whole slide was negative; however subsequent macrodissection to enrich for areas with columnar epithelium resulted in detection of a mutation. In all but one patient, the mutation was in codon 12 of *KRAS*. Fifty-five total specimens with *KRAS* mutations had sufficient normal lung tissue for sequencing, and in every case the adjacent normal lung was found to have a wild type *KRAS* exon 2 sequence.

Overall, *KRAS* p.G12D was the most common mutation and accounted for 67% ($n = 43$) of mutations in CPAMs with MCCs, followed by *KRAS* p.G12V which was detected in 25% ($n = 16$,

Table 1. Clinical, gross, and histologic characteristics of tested CPAMs.

KRAS mutation	c.35 G > A; p.G12D	c.35 G > T; p.G12V	c.34 G > C; p.G12R	c.34 G > T; p.G12C	c.29_31dupGGA; p.G10dup	Wild type	*p* value
Total number of patients	53	21	4	2	1	8	
Gross size of largest cyst (mean ± SD, range)	3 ± 1.5 cm (0.5–6.0)	2.7 ± 1.7 cm (0–6.5)	3.4 ± 1.8 (1.2–5.5)	1.9 ± 2.6 (0–3.7)	0	0.7 ± 0.8 (0–2.5)	3×10^{-3} [a]
Lesions with MCCs	43 (81%)	16 (76%)	3 (75%)	1 (50%)	1 (100%)	0	8.4×10^{-5} [b]
Histologic category							
Type 1	48 (91%)	8 (38%)	0	1 (50%)	0	1 (13%)	
Type 1/3	5 (9%)	9 (43%)	4 (100%)	0	0	1 (13%)	
Type 3	0	4 (19%)	0	1 (50%)	1 (100%)	6 (75%)	8.4×10^{-12} [b]

w weeks, *cGA* corrected gestational age, *SD* standard deviation.
[a]ANOVA.
[b]Fisher exact test.

Table 1). Three lesions had a *KRAS* p.G12R mutation, one lesion had a *KRAS* p.G12C mutation, and one lesion had a duplication of codon 10 (p.G10dup).

Mutant *KRAS* expression in CPAMs

RNAish-based BaseScope™ was utilized to determine the cell type(s) carrying mutant *KRAS*[20]. Using a *KRAS* c.35 G > A specific probe, mutant *KRAS* RNA was found in both mucinous and non-mucinous epithelial cells. A total of six CPAMs were evaluated, including four with clusters of mucinous cells. Mutant *KRAS* RNA was detected in the mucinous cells in all cases, as expected (Supplementary Fig. 1). In all 6 CPAMs, mutant *KRAS* RNA was also detected in non-mucinous cyst epithelium (Fig. 2 and Supplementary Fig. 2) in both larger and smaller cysts, as well as in pneumocytes between cysts (Fig. 2). In one case, a rare mutant signal was detected in possible lesional smooth muscle cells, but at a lower frequency than the wild type probe (Supplementary Fig. 3). In two cases there was a normal appearing airway in the midst of the lesion, and a rare signal of each of the wild type and mutant probes was detected in these airways. In one other case there was a possible normal airway at the periphery of the lesional tissue, and only wild type *KRAS* probe was detected (in very rare cells). The specificity of the probes was confirmed in an adult case of mucinous adenocarcinoma with a *KRAS* p.G12D mutation (Supplementary Fig. 4).

KRAS sequencing of CPAMs without MCCs

We identified 25 additional CPAMs without MCCs but with overall histologic architecture that was similar to that of the CPAMs with MCCs. Ten of these lesions (40%) had a *KRAS* p.G12D mutation, five (20%) had a *KRAS* p.G12V mutation, one had a p.G12R mutation, and one had a p.G12C mutation (Table 1). In contrast to the universal *KRAS* mutations in CPAMs with MCCs, eight CPAMs (32%) without MCCs had a wild type *KRAS* exon 2 sequence. In light of the initial false negative *KRAS* sequencing result for one of the CPAMs with MCCs, these cases and the sequenced blocks were re-reviewed to ensure that there was sufficient columnar epithelium within the macrodissected area. One case had predominantly denuded cyst epithelium throughout all blocks, and the remaining seven cases appeared to have sufficient columnar epithelium in the sequenced area.

Of these eight wild type cases, two were previously reported to have mosaic disease associated mutations in other genes involved in growth and cell cycle regulation (*FGFR2* and *NEK9*)[27,28] which were present in the CPAM as well as in skin lesions. Three other cases with wild type *KRAS* exon 2 had DNA of adequate quantity and quality for NGS analysis (Supplementary Table 2) including the relatively denuded case (115). Several variants of unknown clinical significance were identified, and variants with a VAF between 40 and 60% were presumed to be germline in origin. PCR amplification followed by Sanger sequencing was used to evaluate for each variant with a VAF < 40% within normal lung tissue, and all were also identified in normal lung tissue (Supplementary Table 2). There were no variants with a known clinical significance identified in these three lesions. Additionally, there were no significant copy number variations detected in these cases, although poor DNA quality precluded complete analysis for copy number variations. The remaining three cases with wild type *KRAS* exon 2 had insufficient DNA quantity/quality for additional analysis.

Gross and histologic features of CPAMs with *KRAS* variants

Overall, we identified 89 CPAMs with MCCs or with histologic features similar to those with MCCs. These fell into one of three broad histologic categories (Table 1). Using Dr. Stocker's 2002 histologic classification[2], 65% ($n = 58$) were best classified as a type 1 (large cyst) CPAMs and 13% ($n = 12$) were best classified as

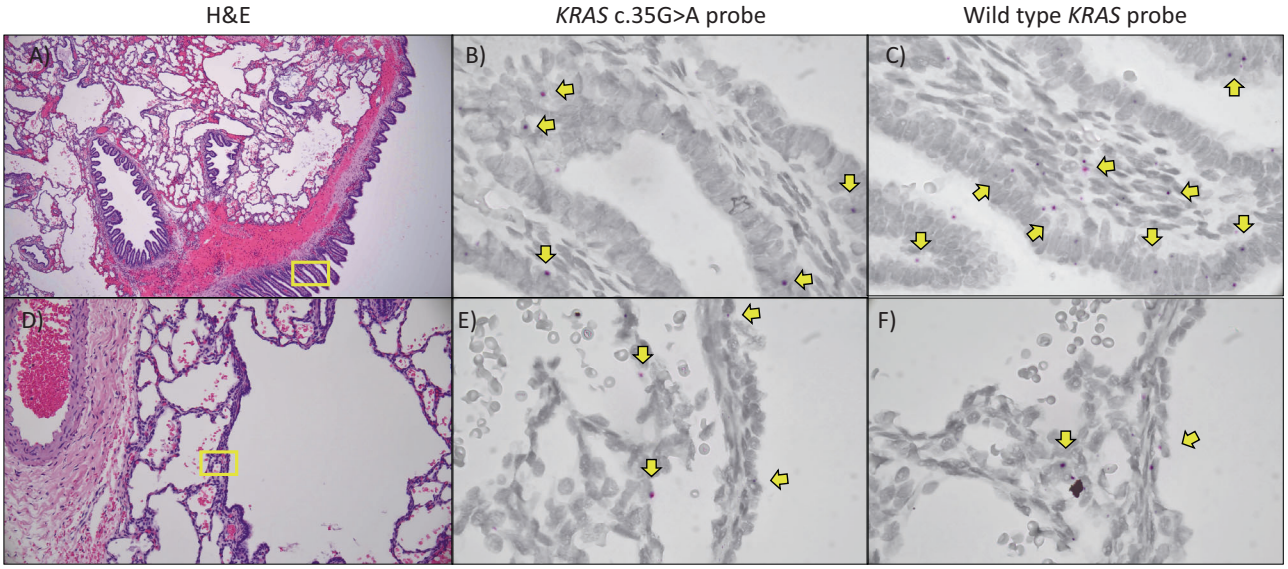

Fig. 2 RNAish-based BaseScope™ in CPAMs detects cells expressing mutant *KRAS*. In an area of non-mucinous cyst epithelium (**A**), both *KRAS* p.G12D (c.35 G > A) (**B**) and wild type *KRAS* (**C**) are detected. In an area of flattened cyst epithelium and alveoli (**D**), both *KRAS* p.G12D (c.35 G > A) (**E**) and wild type *KRAS* (**F**) are identified. RNAish-based BaseScope™ images were all equivalently manipulated to decrease hematoxylin counterstain. The original images are available in Supplementary Fig. 2.

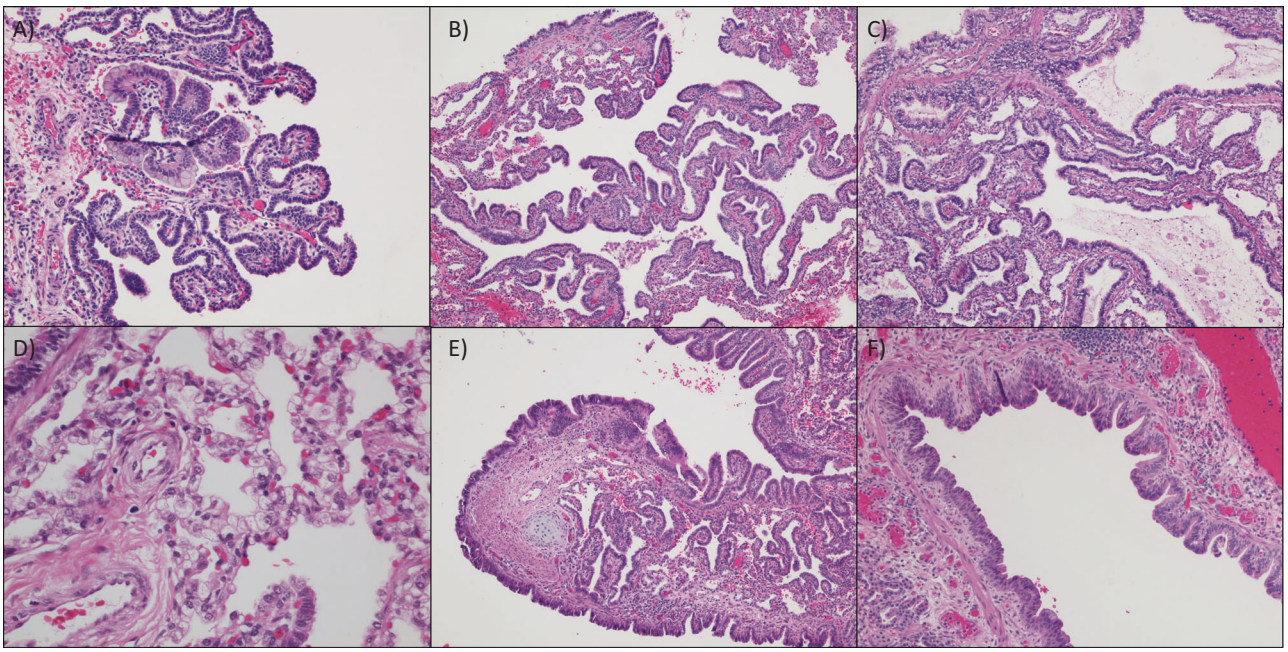

Fig. 3 Shared histologic features in *KRAS*mutated CPAMs. *KRAS* mutated CPAMs demonstrate epithelial complexity (**A**–**C**). Clear pneumocytes with foamy cytoplasm are seen lining alveolar type spaces in a subset of lesions (**D**). Cartilage is occasionally seen within the large cyst wall (**E**). Three cases had large cyst spaces that directly connected with normal airway type epithelium (**F**).

a type 3 (solid/adenomatoid) CPAMs. Twenty-one percent ($n = 19$) fell into an intermediate category with mixed features of both a type 1 and a type 3 CPAM.

Regardless of final classification, all cases had ciliated cuboidal to columnar type epithelium, and many cases demonstrated epithelial complexity (Fig. 3A–C), independent of the histologic category. Overall, 63 cases (72%) demonstrated epithelial complexity, including branching papillary structures and small irregularly shaped spaces. Clear pneumocytes, characterized by foamy vacuolated cytoplasm, were seen lining alveolar type spaces in 24 cases (27%, Fig. 3D). Cartilage was noted in 18% ($n = 16$) of cases (Fig. 3E). There were no statistically significant differences in the frequency of clear pneumocytes or cartilage between histologic categories.

The type 1 CPAMs (Fig. 4) were grossly characterized by readily identifiable cystic spaces measuring an average of 3.2 cm in greatest dimension (Table 2). In eight lesions the largest cyst measured less than 2 cm (the traditionally accepted size cut off for type 1 CPAMs). These lesions with smaller cyst size were histologically indistinguishable from lesions with larger cysts.

The large cyst spaces in these type 1 lesions were always lined by ciliated cuboidal to columnar epithelium with occasional pseudostratification. By definition, type 1 CPAMs universally demonstrated frequent transitions from cysts lined by ciliated

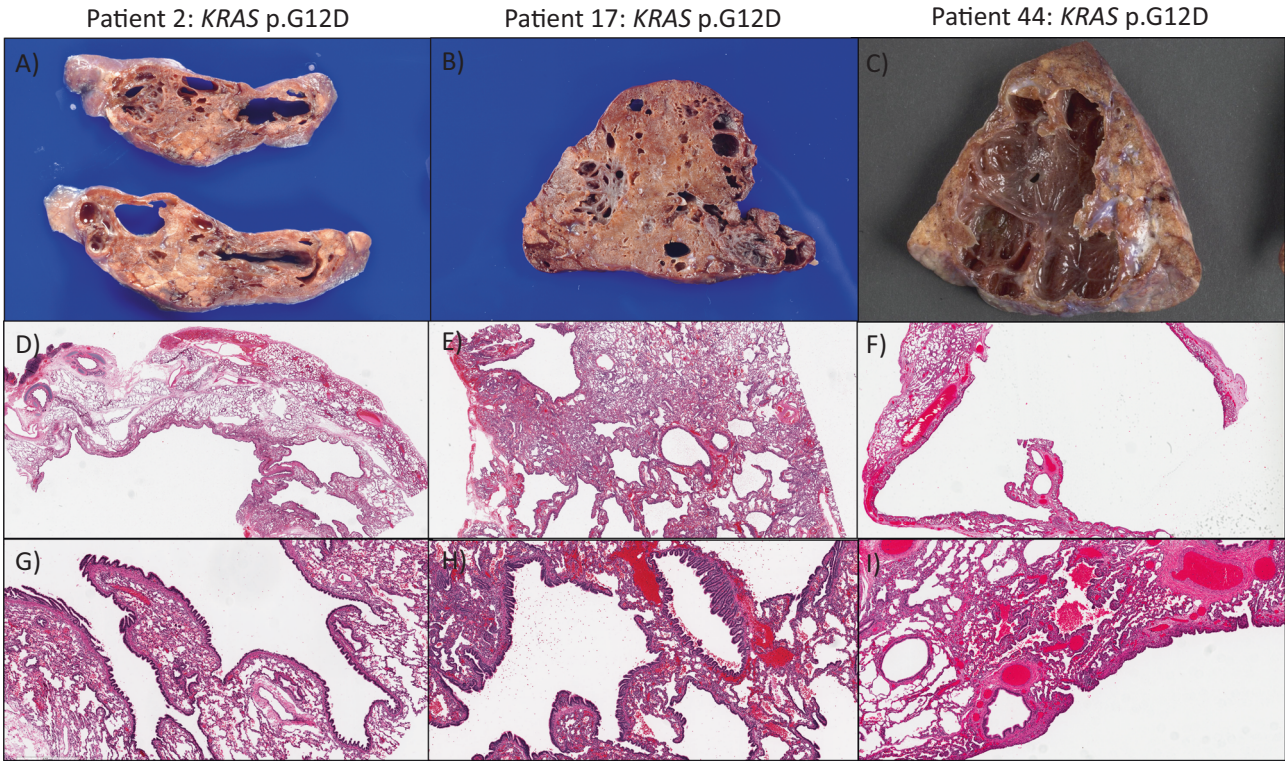

Fig. 4 Gross and histologic features of type 1 CPAMs. Three examples are shown. Grossly, these lesions are defined by large cystic spaces (**A**–**C**). There are numerous abrupt transitions between the large cystic spaces and adjacent alveolar and bronchiolar type spaces (**D**–**F**), and large spaces are lined by ciliated columnar epithelium with occasional pseudostratification (**G**–**I**).

columnar epithelium to adjacent alveolar type spaces, and the cystic spaces were always separated by intervening alveolar type spaces. In three cases, normal airway type epithelium with interspersed goblet cells was observed to directly connect to a large cyst space (Fig. 3F), suggesting that these lesions could be continuous with the normal bronchial tree. Some cysts with a history of a thoracoamniotic shunt showed reactive changes, including squamous metaplasia.

The type 3 CPAMs (Fig. 5) were grossly characterized by single or multiple foci of solid appearing parenchyma with interspersed cystic spaces in eight of twelve cases, measuring an average of 0.4 cm in greatest dimension. There was a statistically significant difference in the largest cyst size between type 1 and type 3 CPAMs ($p = 3.2 \times 10^{-8}$, analysis of variance (ANOVA)).

Histologically, type 3 lesions were characterized by small, irregularly shaped spaces lined by cuboidal to columnar epithelium with ample intervening mesenchyme (Fig. 5). In contrast to type 1 CPAMs, intervening alveolar type spaces were seen in significantly fewer type 3 CPAMs (33%, $n = 4$). Consistent with this, transitions from larger cysts to adjacent alveolar type spaces was rare in these lesions compared to type 1 CPAMs. Additionally, type 3 CPAMs were less likely to show epithelial complexity.

The final subset of CPAMs demonstrated intermediate histologic features and were classified as type 1/3 CPAMs. Grossly, these were characterized by large, readily identifiable cystic spaces with foci of solid appearing parenchyma (Fig. 6). The largest cystic spaces averaged 2.5 cm in greatest dimension, significantly larger than type 3 but similar to pure type 1. In 58% ($n = 11$) the largest cyst measured at least 2 cm in greatest dimension.

Histologically, type 1/3 CPAMs were characterized by large cystic spaces lined by ciliated cuboidal to columnar epithelium with occasional pseudostratification, similar to a type 1. However, they also had foci of back-to-back small, irregularly shaped spaces with cuboidal to low columnar epithelium lining, occasionally with increased mesenchyme, similar to a type 3 CPAM. Complex epithelial projections were common, and cartilage was seen in the wall of one cyst. Intervening alveolar type spaces were seen in most but not all these lesions (79%, $n = 15$). The frequency of transitions from ciliated columnar lined epithelial spaces to alveolar type spaces was more variable than in type 1 and 3 lesions.

Correlation between histologic features and *KRAS* mutation

The *KRAS* mutation distribution differed significantly between lesions in these three histologic categories (Table 1). Ninety-one percent ($n = 48$) of CPAMs with *KRAS* p.G12D mutations had a pure type 1 CPAM morphology, and this mutation was never detected in a type 3 CPAM. This distribution was significantly different from the overall CPAM morphology distribution ($p = 8.4 \times 10^{-12}$, Fisher's exact test), and remained highly significant even when excluding *KRAS* WT cases which were predominantly type 3 ($p = 1.1 \times 10^{-8}$, Fisher's exact test). The histologic features of CPAMs with *KRAS* p.G12V mutations were variable: only 38% ($n = 8$) had a pure type 1 morphology. Of the remaining cases, four (19%) had a pure type 3 morphology and nine had combined type 1/3 morphology (43%).

The specific *KRAS* mutation did not correlate with features of epithelial complexity, presence of foamy pneumocytes or cartilage, or the frequency of mucinous cell clusters. Mucinous cell clusters were never seen in cases with wild type *KRAS* exon 2.

Of the eight cases with a wild type *KRAS* exon 2, only one had a pure type 1 morphology. This type 1 CPAM had predominantly denuded epithelium, which may have precluded identification of a *KRAS* variant. Of the remaining seven wild type cases, one was of mixed type 1/3 morphology and seven were pure type 3. Type 3 CPAMs with *KRAS* mutations were histologically indistinguishable from CPAMs with wild type *KRAS* exon 2. In two of these cases, mutations in alternate genes were previously identified (*FGFR2*

Table 2. Defining gross and histologic features of type 1, 3, and 1/3 CPAMs.

Histologic category	*n*	Largest cyst size cm (mean ± SD, range)	Intervening alveolar type spaces	Frequent transitions	Complexity
1	58	3.2 ± 1.4 (0.5–6.0)	58 (100%)	57 (98%)	42 (74%)
3	12	0.4 ± 0.5 (0–1.4)	4 (33%)	2 (17%)	5 (42%)
1/3	19	2.5 ± 1.6 (0.6–6.5)	15 (79%)	15 (78%)	16 (84%)
p value		6.4×10^{-8} [a]	1.6×10^{-8} [b]	3.2×10^{-12} [b]	4.7×10^{-2} [b]

SD standard deviation.
[a]ANOVA.
[b]Fisher exact test.

and *NEK9*)[27,28], suggesting that a subset of type 3 and type 1/3 CPAMs may harbor driver mutations in alternate genes.

Clinical characteristics of patients with *KRAS* mutated CPAMs

Patients with *KRAS* mutated CPAMs had an average corrected gestational age at surgery of 38 weeks, and a male to female ratio of 1.25:1. There was no correlation between mutation and corrected gestational age at surgery. Six patients died within one month of birth due to complications of pulmonary hypoplasia and/or prematurity.

Patient charts were reviewed for features potentially associated with mosaic RASopathy. One patient had an extensive lymphatic malformation, which can be associated with *KRAS* mutations[29]. However, the patient died at 10 months of age and additional tissue sampling was not performed. One patient developed neuroblastoma at 10 months of age, which can also harbor *KRAS* mutations[30]. However, sequencing of the neuroblastoma biopsy showed a wild type *KRAS* exon 2. Additionally, two patients were noted to have nevi, which can be associated with mosaic RASopathy[31], but those lesions have not been biopsied

DISCUSSION

Our study contrasts with older literature and shows that all MCCs arising in CPAMs have activating *KRAS* mutations, and that the same mutation is seen not only in all MCCs within a single patient but also within non-mucinous lesional epithelium. *KRAS* mutations were also seen in 17 of 25 (68%) type 1, type 3, or type 1/3 CPAMs without MCCs. Our findings are consistent with other smaller studies that have also shown *KRAS* mutations to be present in most type 1 CPAMs as well as in a smaller percentage of lesions with smaller cysts[15].

Numerous CPAM classification schemes have been proposed involving both cyst size and morphology[1–4], and classification remains somewhat subjective, with limited published images available to appreciate the full spectrum of morphology. Depending on the applied classification scheme, some of our lesions may have been categorized as type 2/small cyst or type 3/cystic adenomatoid in the past[2,3], or they may have been categorized following a fetal classification scheme[4], but morphologically they all demonstrate a spectrum of findings suggesting excessive airway epithelial tissue, and in our opinion they are distinct from the typical morphology of type 2 cases associated with features of obstruction[11]. We have never seen mucinous cells in classic type 2 cases. Despite many pathologists' efforts at accurate classification, the spectrum of overlapping morphology between type 1 and type 3 lesions in our series is consistent with historical studies showing lack of a clear cut off between solid, small cyst, and large cyst malformations[32]. Furthermore, the overlapping *KRAS* mutation spectrum and histology shared by these lesions is not consistent with the longstanding hypothesis that type 3 CPAMs are a localized form of pulmonary hyperplasia[3].

The presence of a *KRAS* mutation driving non-mucinous CPAM epithelial proliferation is consistent with our prior work demonstrating a high mitotic rate in CPAM epithelium in infants[17]. Infant lung in general is more proliferative than adult lung, but analysis showed that the rate of proliferation of infant mucinous cells correlated with that of non-mucinous CPAM-type epithelium but not with non-lesional infant airway epithelium. In addition, previous in vitro work has shown that CPAM-derived epithelial cells have a cell-autonomous growth advantage compared to control epithelium in three-dimensional lung organoid culture[33].

Prior studies suggested that airway obstruction may underlie many congenital lung malformations (particularly type 2 CPAMs), but detailed subclassification was often not provided. The current work and our prior observations suggest that *KRAS* mutations are driving CPAM development in most cases of type 1 and type 3 lesions. Two other series have suggested mucinous cells and/or *KRAS* mutations may be present in a small number of type 2 CPAMS[15,34]. However, beyond cyst size the histologic criteria for classification are poorly defined. Evaluation of *KRAS* mutations in cases we considered to be classic type 2 CPAMs and in morphologically related intra-lobar and extra-lobar sequestrations was beyond the scope of this study, but certainly some cases included here had intermediate sized cysts (Tables 1 and 2). We favor the hypothesis that the pathogenesis of these lesions is distinct from that of bronchial atresia-related type 2 lesions, but this hypothesis and the identification of reproducible histologic features to classify CPAMs based on pathogenetic mechanism rather than cyst size is an area that requires additional investigation.

Abundant murine studies support the idea that airway epithelial mutations can lead to abnormal parenchymal development when they are introduced early in development. When $Kras^{G12D}$ is expressed in embryonic mouse lungs, it results in diffusely cystic parenchyma with complex architecture reminiscent of type 1 CPAMs[35]. In contrast, knock-in expression of other, more weakly activating, *Kras* mutations have been shown to have normal or only mildly enlarged airspaces[36,37]. Over-expression of growth factors including *FGF7*[38] or *Fgf10*[39], overexpression of transcription factor *Sox2*[40], or mesenchymal deletion of the TGF beta receptor (*Tgfbr2*)[41] can result in similar abnormal cystic lung development. Mutations affecting genes other than *KRAS* may represent alternative pathways of CPAM development in a subset of cases, including the eight cases with a wild type *KRAS* exon 2 in the current study.

The overall *KRAS* mutation distribution in our study is similar to what has been previously reported in mucinous cells within CPAMs[34], and in non-mucinous lesional tissue[15], with *KRAS* p.G12D and p.G12V being the most common mutations. Although *KRAS* p.G12C is the most common mutation overall in lung adenocarcinomas in adults, p.G12D and p.G12V are more common in mucinous lung adenocarcinoma, and these amino acid substitutions therefore seem to be closely linked to this morphology[26,42]. Although we do not believe the specific amino acid substitution is diagnostically defining, the significant correlation between the

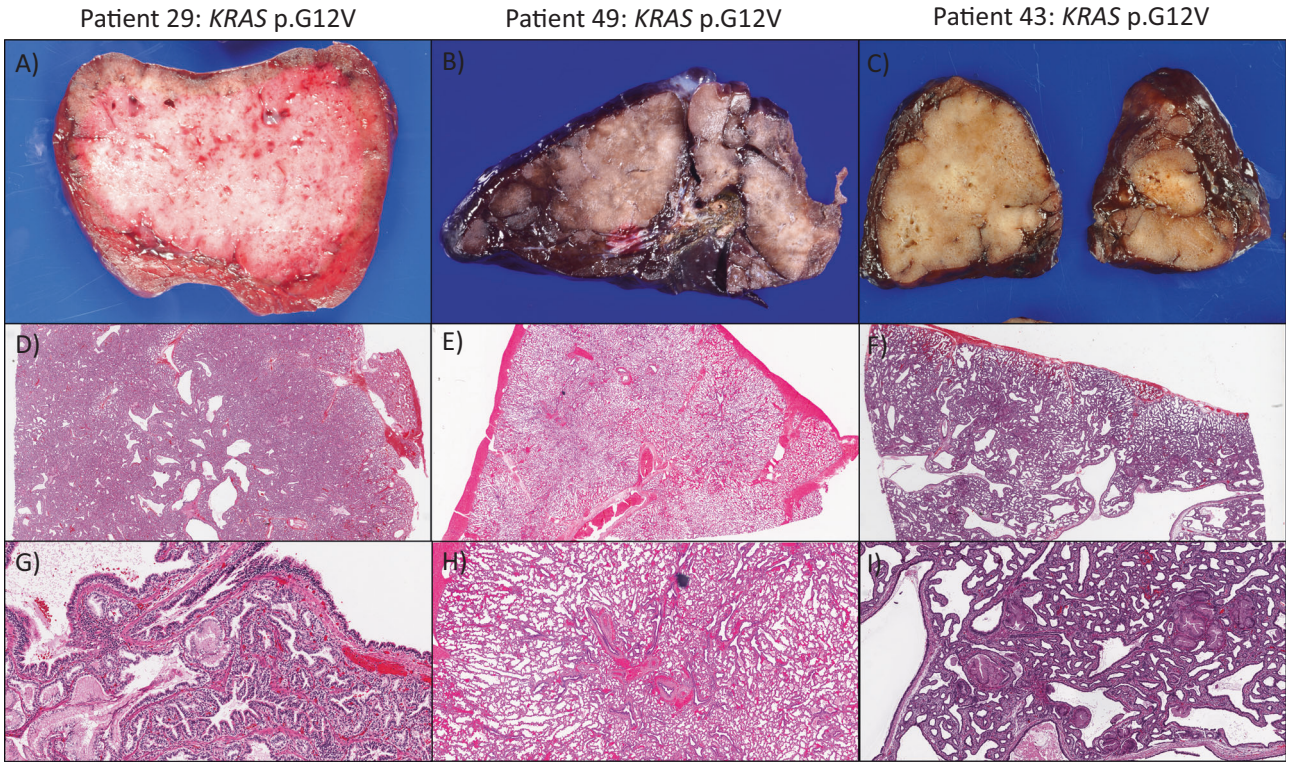

Fig. 5 Gross and histologic features of type 3 CPAMs. Three examples are shown. Grossly, these lesions are predominantly solid in appearance with occasional small cystic spaces (**A**–**C**). Histologically, they are characterized by a somewhat solid appearance at low power with no visible alveolar type spaces within the lesion (**D**–**F**) and consist of small irregularly shaped spaces lined by low columnar epithelium with ample intervening mesenchyme (**G**–**I**).

KRAS p.G12D mutation and type 1 morphology in comparison to other *KRAS* mutations is consistent with this mutation acting as a driver of the malformation. Biochemical activity, in vitro signaling potential, and cancer outcomes[43] are among the features that may vary depending on the specific amino acid substitution at this location, and it is reasonable to assume that different mutations could have slightly different signaling effects even if they arise at the same time and in the same cell type during embryonic lung development. The only *KRAS* mutation we detected outside of codon 12 was one case of *KRAS* p.G10dup. This mutation has been reported predominantly in hematolymphoid and colon cancers[44,45], and has been shown to be highly activating in vitro and in cell cultures[46,47], consistent with an activating role.

In addition to biochemical activity, the variation in morphology of CPAMs could be due to the timing or location at which the *KRAS* mutation occurs. One murine model with *Fgf10* overexpression noted marked variability in lung morphology even within a single litter, which the authors suggested could be due to location, timing or extent of transgene expression[39]. This is consistent with another model of targeted *Fgf10* expression via timed adenoviral vector injection resulting in localized malformations in which morphology depended on timing and location of injection[48]. Similarly, the morphology of cysts in mice with *Sox2* overexpression is dependent on the timing during development[40]. A third possibility is that alternative mutations (such as the *FGFR2* or *NEK9* mutations previously reported in two of our patients[27,28]) could account for differences in morphology. Additional studies will be required to determine how widespread the presence of *KRAS* mutations is in the various other types of CPAMs or in sequestrations with CPAM-type maldevelopment.

The identification of a subset of CPAMs as a developmental anomaly related to aberrant RAS signaling places these lesions in a growing field of RAS mosaic disorders ("RASopathies"). Germline mutations affecting the RAS/MAPK signaling pathway do not include the highly oncogenic codon 12 *KRAS* mutations[49], likely due to devastating early developmental consequences. However, codon 12 mutations are detected in mosaic RASopathies that are characterized predominantly by various patterns of nevi[31]. Associated abnormalities in other organ systems are increasingly reported in these patients, including overgrowth and vascular malformations[50]. Recently, arteriovenous malformations in the brain have been reported to contain somatic *KRAS* codon 12 mutations within endothelial cells[51], and this expression is sufficient to drive vascular malformations in animal models[52]. Despite identification of "oncogenic" *KRAS* mutations, these mosaic disorders have not yet been broadly reclassified as neoplasms—the mutation is present in only a subset of cells, and at least in the case of CPAMs, the lesions do not continue to grow outside of fetal life. CPAMs therefore still fit in the category of a malformation as defined as a non-progressive congenital anomaly due to an alteration in the primary developmental program[53]. As molecular drivers of malformations continue to be identified, it is possible that existing definitions of morphology will be updated. In contrast to the CPAM lesion as a whole, the clusters of mucinous cells, which are clonal, are more clearly identifiable as a classic neoplastic process.

Many diagnostic terms have been proposed for these small clusters of mucinous cells, ranging from hyperplasia to metaplasia to minimally invasive mucinous adenocarcinoma. In contrast to the adult mucinous adenocarcinomas evaluated here and those reported in the literature[26,42], we did not detect other genetic mutations in the MCCs of infants, and late metastases have not been reported with documented complete resection. We previously characterized the histologic features of 671 MCCs from 44 infantile CPAMs, all of which were included in the current study, and found that they are histologically indistinguishable from adult minimally invasive mucinous adenocarcinomas[17]. However, despite the histologic similarities, including multifocality

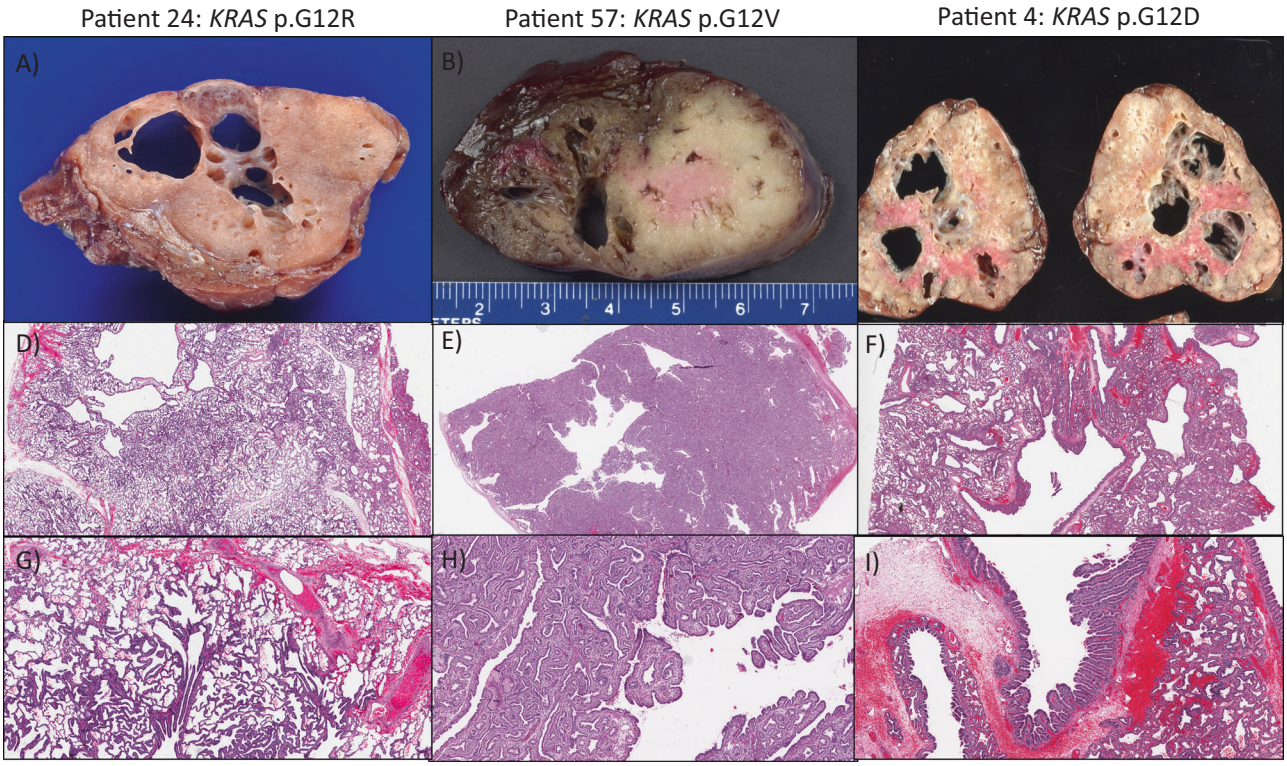

Fig. 6 Gross and histologic features of type 1/3 CPAMs. Three examples are shown. Grossly, these lesions consist of solid appearing parenchyma with admixed larger cystic spaces (**A**–**C**). The low power appearance is heterogenous, with more solid appearing areas intermixed with large cysts and relatively normal appearing alveolar type spaces (**D**–**F**). Larger cysts are lined by ciliated columnar epithelium, similar to a type 1, while more solid appearing areas demonstrate increased mesenchyme, similar to a type 3 (**G**–**I**).

and growth patterns that could be considered invasive in an adult, these lesions have a benign clinical course when entirely resected in infancy. We therefore continue to avoid using "carcinoma" in infants to avoid the physical harms of over-treatment. For consistency we have used the descriptive term "mucinous cell clusters" here, but other terms involving atypia, or perhaps adenoma may be equally valid. In the two CPAMs from children over a year of age, the MCCs remained minute, and this lack of progression would support the use of less aggressive terminology.

Disparate foci of mucinous adenocarcinoma in adults appear to be clonally related in most instances[26], presumably due to aerogenous spread. A similar process may occur in infants, but given the developmental setting, it is difficult to draw a direct comparison. Because MCCs in CPAMs are arising in a background of widespread mosaic *KRAS* mutated cells, it is impossible to determine whether each mucinous cluster is arising independently sometime after lesion formation. And if they are not arising independently, their spread within the lesion may be related to normal developmental migration rather than representing malignant intra-airspace metastasis.

Our BaseScope™ data suggests that the mutant *KRAS* is primarily localized in the epithelial component of the CPAM. It was more easily detected in airway type epithelium but was also occasionally present in pneumocytes. Unfortunately, not every signal can be confidently assigned to a specific cell type, and this technique is limited to detecting cells expressing the mutant allele at the time of resection. It therefore does not necessarily reflect the relative percentages of each cell containing a mutant allele and cannot entirely exclude the presence of the allele in other cell types. The lack of sensitivity also precludes using this technique to further confirm the absence of mutant cells in the morphologically uninvolved lung. Thus, identifying the cellular origin of *KRAS*-driven cystic lesions proves difficult. Nevertheless, we did observe *KRAS* mutations in rare alveolar cells and cuboidal pneumocytes between cysts, suggesting a potential cellular origin for CPAMs similar to that of lung adenocarcinomas: Type 2 pneumocytes, club cells, and multiciliated cells have all been proposed as the cell of origin for *KRAS*-driven lung adenocarcinomas[54–56].

Among our patients, *KRAS* mutations outside of the CPAM have not been detected. One patient with a lymphovascular malformation was very suspicious for further involvement, but an autopsy was not performed, and mosaicism could not be established. Mosaicism has only been established for two CPAMs that were wild type for *KRAS* but had mutations in other genes. Six other cases also had a wild type *KRAS* exon 2 sequence, and sequencing of three of these CPAMs revealed multiple variants of uncertain clinical significance (Supplementary Table 2). *KRAS* variants within MCC in CPAMs had a VAF of less than 35% (Supplementary Table 1), and we would expect other potential driver mutations to have VAFs within a similar range. Sanger sequencing was used to evaluate normal lung tissue for all variants with a VAF of less than 40%, and all variants were also found within normal lung, supporting a germline origin. All other identified variants had a VAF between 40 and 60%, consistent with a germline origin. It is possible that *KRAS* mutations may be present in these lesions at a level below the limit of detection of our assay. Additionally, our NGS panel was primarily designed to evaluate pediatric cancers, and it may not cover all genes that could play a role in driving these malformations. Poor archival DNA quality prevented further search for other driver mutations in the remaining three cases.

Traditionally, at our institution, we recommend a complete lobectomy for all CPAMs independent of Stocker type (which cannot be definitively established prior to resection) and independent of the presence or absence of symptoms in order to reduce the risk of CPAM associated pneumonia and

adenocarcinoma in the future. There are reports of metastatic mucinous adenocarcinoma arising in CPAMs that were either not resected or were incompletely resected in infancy[57–63], including a report of sarcomatoid change in metastatic mucinous adenocarcinoma arising in an adult with an unresected CPAM[64]. The presence of *KRAS* mutations in a subset of lesions lends support to complete surgical resection to minimize this oncologic risk in the future. Although genetic testing to confirm the presence or absence of a *KRAS* mutation in resected CPAM tissue provides important etiologic (pathologic) insight and lends support to the current management recommendations, the clinical utility of routine *KRAS* genetic testing remains uncertain. Our findings demonstrate that the presence of mucinous cells or a typical Stocker type 1 large cyst morphology is an extremely strong surrogate marker for this mutation. Similarly, in cases with MCCs (76% of type 1 CPAMs in the current study), a minimum of a lobectomy and complete resection of the lesion have already been advocated[17]. The findings of the current study further support this recommendation highlighting the need for a lobectomy for complete resection of all Stocker type 1 lesions, regardless of the identification of MCCs. The presence of cells expressing mutant *KRAS* RNA outside of bronchiolar-type epithelium suggests that in subtotal resections the margins cannot be confidently assessed by histology alone. Genetic testing of lesional tissue might be helpful if the classification is uncertain and if the definitive presence of a *KRAS* mutation would affect recommendations for further surgery (if resection did not occur by lobectomy or if the lesion involves a second lobe), or if the patient has other congenital anomalies that could represent part of a mosaic disorder. Problematically, however, the absence of a *KRAS* codon 12 mutation would not exclude other, possibly weaker *KRAS* mutations or mutations in alternative genes such as in *FGFR2*. Not all features of RASopathy may be present at birth, but rare reported cases of codon 12 mutations have had severe phenotypes that are unlikely to be overlooked[65–68].

If genetic testing is undertaken, care should be taken to specifically isolate lesional tissue containing abundant airway type epithelium and to use an assay with high sensitivity. Early studies testing for *KRAS* mutations in type 1 CPAMs were negative[69], and it may be either that we have selected for a higher percentage of lesional cells or that our assay is more sensitive. In one case where we initially did not macrodissect areas enriched in columnar cells we obtained a false negative result. Our methods here do not allow assessment of allele frequency in most specimens, but in those submitted for NGS (estimated to contain between 15 and 40% mucinous cells), VAF ranged from 20–33%. In other recent studies[15] *KRAS* codon 12 mutations were found in relatively similar frequencies in both mucinous (24–55%) and non-mucinous (6–43%) foci.

The identification of *KRAS* mutations outside of MCCs may explain the late development of metastatic mucinous adenocarcinoma in infants with incompletely resected lesions. Rather than a metastasis from one of the resected minute clusters of mucinous cells, these late lesions could equally likely be due to a new lesion arising from residual lung parenchyma with widespread *KRAS* mutation. Two reports exist of patients with CPAMs and metastatic mucinous adenocarcinoma who had acquired *GNAS* p.R201C mutations in the metastatic lesion in addition to the original *KRAS* p.G12V in the primary site[34,70], suggesting that additional mutations may be necessary for the development of carcinoma in these patients. This further emphasizes the importance of complete resection via a lobectomy rather than a symptomatic cystectomy that may leave behind subtle areas of abnormalities including cells carrying the *KRAS* mutation.

Some case reports have suggested arbitrarily increased post-surgical CT imaging of patients with *KRAS* mutations outside of the MCCs[71]. Our results suggest that *KRAS* mutation is a near universal phenomena in type 1 CPAMs. These often have complex architecture, including papillary structures[17]. Detection of a *KRAS* mutation does not change the historic lack of aggressive behavior in appropriately resected lesions in infants[17]. In our institution, post-resection CT imaging with its concomitant exposure to radiation, is not performed in infants or young children that have undergone a lobectomy for a CPAM independent of the presence of MCC and/or identification of *KRAS* mutations.

DATA AVAILABILITY

The datasets generated and/or analyzed during the current study are available from the corresponding author on reasonable request.

REFERENCES

1. Stocker, JT, Madewell, JE & Drake, RM. Congenital cystic adenomatoid malformation of the lung. Classification and morphologic spectrum. Hum Pathol 8, 155–171 (1977).
2. Stocker, J. Congenital pulmonary airway malformation: A new name for and an expanded classification of congenital cystic adenomatoid malformation of the lung. Symposium 24: Non-neoplastic Lung Disease. Histopathology 41, 424–430 (2002).
3. Langston, C. New concepts in the pathology of congenital lung malformations. Semin Pediatr Surg 12, 17–37 (2003).
4. Kreiger, PA, Ruchelli, ED, Mahboubi, S, Hedrick, H, Scott Adzick, N & Russo, PA. Fetal pulmonary malformations: defining histopathology. Am J Surg Pathol 30, 643–649 (2006).
5. Dehner, LP, Messinger, YH, Schultz, KAP, Williams, GM, Wikenheiser-Brokamp, K & Hill, DA. Pleuropulmonary Blastoma: Evolution of an Entity as an Entry into a Familial Tumor Predisposition Syndrome. Pediatr Dev Pathol 18, 504–511 (2015).
6. Messinger, YH, Stewart, DR, Priest, JR, Williams, GM, Harris, AK, Schultz, KAP et al. Pleuropulmonary blastoma: A report on 350 central pathology–confirmed pleuropulmonary blastoma cases by the International Pleuropulmonary Blastoma Registry. Cancer 121, 276–285 (2015).
7. Szafranski, P, Coban-Akdemir, ZH, Rupps, R, Grazioli, S, Wensley, D, Jhangiani, SN et al. Phenotypic expansion of TBX4 mutations to include acinar dysplasia of the lungs. Am J Med Genet A 170, 2440–2444 (2016).
8. Vincent, M, Karolak, JA, Deutsch, G, Gambin, T, Popek, E, Isidor, B et al. Clinical, Histopathological, and Molecular Diagnostics in Lethal Lung Developmental Disorders. Am J Respir Crit Care Med 200, 1093–1101 (2019).
9. Kunisaki, SM, Fauza, DO, Nemes, LP, Barnewolt, CE, Estroff, JA, Kozakewich, HP et al. Bronchial atresia: the hidden pathology within a spectrum of prenatally diagnosed lung masses. J Pediatr Surg 41, 61–65; discussion 61-65 (2006).
10. Riedlinger, WFJ, Vargas, SO, Jennings, RW, Estroff, JA, Barnewolt, CE, Lillehei, CW et al. Bronchial atresia is common to extralobar sequestration, intralobar sequestration, congenital cystic adenomatoid malformation, and lobar emphysema. Pediatr Dev Pathol 9, 361–373 (2006).
11. Pogoriler, J, Swarr, D, Kreiger, P, Adzick, NS & Peranteau, W. Congenital Cystic Lung Lesions: Redefining the Natural Distribution of Subtypes and Assessing the Risk of Malignancy. Am J Surg Pathol 43, 47–55 (2019).
12. Lantuejoul, S, Nicholson, AG, Sartori, G, Piolat, C, Danel, C, Brabencova, E et al. Mucinous cells in type 1 pulmonary congenital cystic adenomatoid malformation as mucinous bronchioloalveolar carcinoma precursors. Am J Surg Pathol 31, 961–969 (2007).
13. Kim, M-Y, Kang, CH & Park, S-H. Multifocal synchronous mucinous adenocarcinomas arising in congenital pulmonary airway malformation: a case report with molecular study. Histopathology 65, 926–932 (2014).
14. Rossi, G, Gasser, B, Sartori, G, Migaldi, M, Costantini, M, Mengoli, MC et al. MUC5AC, cytokeratin 20 and HER2 expression and K-RAS mutations within mucinogenic growth in congenital pulmonary airway malformations. Histopathology 60, 1133–1143 (2012).
15. Hermelijn, SM, Wolf, JL, Dorine den Toom, T, Wijnen, RMH, Rottier, RJ, Schnater, JM et al. Early KRAS oncogenic driver mutations in nonmucinous tissue of congenital pulmonary airway malformations as an indicator of potential malignant behavior. Hum Pathol 103, 95–106 (2020).
16. Fakler, F, Aykutlu, U, Brcic, L, Eidenhammer, S, Thueringer, A, Kashofer, K et al. Atypical goblet cell hyperplasia occurs in CPAM 1, 2, and 3, and is a probable precursor lesion for childhood adenocarcinoma. Virchows Arch 476, 843–854 (2020).
17. Nelson, ND, Litzky, LA, Peranteau, WH & Pogoriler, J. Mucinous Cell Clusters in Infantile Congenital Pulmonary Airway Malformations Mimic Adult Mucinous Adenocarcinoma But Are Not Associated With Poor Outcomes When Appropriately Resected. Am J Surg Pathol 44, 1118–1129 (2020).

18. Surrey, LF, MacFarland, SP, Chang, F, Cao, K, Rathi, KS, Akgumus, GT et al. Clinical utility of custom-designed NGS panel testing in pediatric tumors. Genome Medicine 11, 32 (2019).
19. Integrative genomics viewer | Nature Biotechnology. https://www.nature.com/articles/nbt.1754.
20. Baker, A-M, Huang, W, Wang, X-MM, Jansen, M, Ma, X-J, Kim, J et al. Robust RNA-based in situ mutation detection delineates colorectal cancer subclonal evolution. Nat Commun 8, 1998 (2017).
21. RStudio Team. *RStudio: Integrated Development Environment for R*. (Rstudio, PBC, 2021).
22. Wickham, H, Averick, M, Bryan, J, Chang, W, McGowan, LD, François, R et al. Welcome to the Tidyverse. Journal of Open Source Software 4, 1686 (2019).
23. Kassambara, A. *rstatix: Pipe-Friendly Framework for Basic Statistical Tests*. (2021).
24. Ichinokawa, H, Ishii, G, Nagai, K, Kawase, A, Yoshida, J, Nishimura, M et al. Distinct clinicopathologic characteristics of lung mucinous adenocarcinoma with KRAS mutation. Hum Pathol 44, 2636–2642 (2013).
25. Kadota, K, Yeh, Y-C, D'Angelo, SP, Moreira, AL, Kuk, D, Sima, CS et al. Associations between mutations and histologic patterns of mucin in lung adenocarcinoma: invasive mucinous pattern and extracellular mucin are associated with KRAS mutation. Am J Surg Pathol 38, 1118–1127 (2014).
26. Yang, S-R, Chang, JC, Leduc, C, Tan, KS, Dogan, S, Benayed, R et al. Invasive Mucinous Adenocarcinomas With Spatially Separate Lung Lesions: Analysis of Clonal Relationship by Comparative Molecular Profiling. J Thorac Oncol 16, 1188–1199 (2021).
27. Sheppard, SE, Smith, A, Grand, K, Pogoriler, J, Rubin, AI, Schindewolf, E et al. Further delineation of the phenotypic spectrum of nevus comedonicus syndrome to include congenital pulmonary airway malformation of the lung and aneurysm. Am J Med Genet A 182, 746–754 (2020).
28. Linn, R, Sheppard, S, Burrill, N, Oliver, E, Izumi, K, Campbell, I et al. Prenatally identified Schimmelpenning Syndrome with cystic pulmonary airway malformation: not a coincidental finding. in *40th Annual David W. Smith Workshop on Malformations and Morphogenesis* (2019).
29. Sevick-Muraca, EM & King, PD. Lymphatic Vessel Abnormalities Arising from Disorders of Ras Signal Transduction. Trends Cardiovasc Med 24, 121–127 (2014).
30. Mlakar, V, Morel, E, Mlakar, SJ, Ansari, M & Gumy-Pause, F. A review of the biological and clinical implications of RAS-MAPK pathway alterations in neuroblastoma. J Exp Clin Cancer Res 40, 1–16 (2021).
31. Hafner, C & Groesser, L. Mosaic RASopathies. Cell Cycle 12, 43–50 (2013).
32. Bale, PM. Congenital Cystic Malformation of the Lung: A Form of Congenital Bronchiolar ("Adenomatoid") Malformation. Am J Clin Pathol 71, 411–420 (1979).
33. Swarr, DT, Peranteau, WH, Pogoriler, J, Frank, DB, Adzick, NS, Hedrick, HL et al. Novel Molecular and Phenotypic Insights into Congenital Lung Malformations. Am J Respir Crit Care Med 197, 1328–1339 (2018).
34. Chang, W, Zhang, YZ, Wolf, JL, Hermelijn, SM, Schnater, JM, Thüsen, JH et al. Mucinous adenocarcinoma arising in congenital pulmonary airway malformation: clinicopathological analysis of 37 cases. Histopathology 78, 434–444 (2021).
35. Shaw, AT, Meissner, A, Dowdle, JA, Crowley, D, Magendantz, M, Ouyang, C et al. Sprouty-2 regulates oncogenic K-ras in lung development and tumorigenesis. Genes & Development 21, 694–707 (2007).
36. Wong, JC, Perez-Mancera, PA, Huang, TQ, Kim, J, Grego-Bessa, J, del pilar Alzamora, M et al. KrasP34R and KrasT58I mutations induce distinct RASopathy phenotypes in mice. JCI Insight 5, e140495.
37. Hernández-Porras, I, Fabbiano, S, Schuhmacher, AJ, Aicher, A, Cañamero, M, Cámara, JA et al. K-RasV14I recapitulates Noonan syndrome in mice. Proc Natl Acad Sci U S A 111, 16395–16400 (2014).
38. Simonet, WS, DeRose, ML, Bucay, N, Nguyen, HQ, Wert, SE, Zhou, L et al. Pulmonary malformation in transgenic mice expressing human keratinocyte growth factor in the lung. Proceedings of the National Academy of Sciences 92, 12461–12465 (1995).
39. Clark, JC, Tichelaar, JW, Wert, SE, Itoh, N, Perl, AK, Stahlman, MT et al. FGF-10 disrupts lung morphogenesis and causes pulmonary adenomas in vivo. Am J Physiol Lung Cell Mol Physiol 280, L705-715 (2001).
40. Ochieng, JK, Schilders, K, Kool, H, Boerema-De Munck, A, Buscop-Van Kempen, M, Gontan, C et al. Sox2 Regulates the Emergence of Lung Basal Cells by Directly Activating the Transcription of Trp63. Am J Respir Cell Mol Biol 51, 311–322 (2014).
41. Miao, Q, Chen, H, Luo, Y, Chiu, J, Chu, L, Thornton, ME et al. Abrogation of mesenchyme-specific TGF-β signaling results in lung malformation with prenatal pulmonary cysts in mice. Am J Physiol Lung Cell Mol Physiol 320, L1158–L1168 (2021).
42. Chang, JC, Offin, M, Falcon, C, Brown, D, Houck-Loomis, BR, Meng, F et al. Comprehensive Molecular and Clinicopathologic Analysis of 200 Pulmonary Invasive Mucinous Adenocarcinomas Identifies Distinct Characteristics of Molecular Subtypes. Clin Cancer Res 27, 4066–4076 (2021).
43. Haigis, KM. KRAS Alleles: The Devil Is in the Detail. Trends Cancer 3, 686–697 (2017).
44. Tate, JG, Bamford, S, Jubb, HC, Sondka, Z, Beare, DM, Bindal, N et al. COSMIC: the Catalogue Of Somatic Mutations In Cancer. Nucleic Acids Research 47, D941–D947 (2019).
45. Mutation overview page KRAS - p.G10dup (Insertion - In frame). https://cancer.sanger.ac.uk/cosmic/mutation/overview?id=99228974.
46. Tong, JHM, Lung, RWM, Sin, FMC, Law, PPY, Kang, W, Chan, AWH et al. Characterization of rare transforming KRAS mutations in sporadic colorectal cancer. Cancer Biol Ther 15, 768–776 (2014).
47. Bollag, G, Adler, F, elMasry, N, McCabe, PC, Conner, E, Thompson, P et al. Biochemical Characterization of a Novel KRAS Insertion Mutation from a Human Leukemia*. Journal of Biological Chemistry 271, 32491–32494 (1996).
48. Gonzaga, S, Henriques-Coelho, T, Davey, M, Zoltick, PW, Leite-Moreira, AF, Correia-Pinto, J et al. Cystic adenomatoid malformations are induced by localized FGF10 overexpression in fetal rat lung. Am J Respir Cell Mol Biol 39, 346–355 (2008).
49. Guerrero, S, Casanova, I, Farré, L, Mazo, A, Capellà, G & Mangues, R. K-ras codon 12 mutation induces higher level of resistance to apoptosis and predisposition to anchorage-independent growth than codon 13 mutation or proto-oncogene overexpression. Cancer Res 60, 6750–6756 (2000).
50. Chang, CA, Perrier, R, Kurek, KC, Estrada-Veras, J, Lehman, A, Yip, S et al. Novel findings and expansion of phenotype in a mosaic RASopathy caused by somatic KRAS variants. Am J Med Genet A 185, 2829–2845 (2021).
51. Nikolaev, SI, Vetiska, S, Bonilla, X, Boudreau, E, Jauhiainen, S, Rezai Jahromi, B et al. Somatic Activating KRAS Mutations in Arteriovenous Malformations of the Brain. New England Journal of Medicine 378, 250–261 (2018).
52. Park, ES, Kim, S, Huang, S, Yoo, JY, Körbelin, J, Lee, TJ et al. Selective Endothelial Hyperactivation of Oncogenic KRAS Induces Brain Arteriovenous Malformations in Mice. Ann Neurol 89, 926–941 (2021).
53. Hennekam, RC, Biesecker, LG, Allanson, JE, Hall, JG, Opitz, JM, Temple, IK et al. Elements of morphology: general terms for congenital anomalies. Am J Med Genet A 161A, 2726–2733 (2013).
54. Sutherland, KD, Song, J-Y, Kwon, MC, Proost, N, Zevenhoven, J & Berns, A. Multiple cells-of-origin of mutant K-Ras-induced mouse lung adenocarcinoma. Proc Natl Acad Sci U S A 111, 4952–4957 (2014).
55. Mainardi, S, Mijimolle, N, Francoz, S, Vicente-Dueñas, C, Sánchez-García, I & Barbacid, M. Identification of cancer initiating cells in K-Ras driven lung adenocarcinoma. Proc Natl Acad Sci U S A 111, 255–260 (2014).
56. Kim, N, Kim, HK, Lee, K, Hong, Y, Cho, JH, Choi, JW et al. Single-cell RNA sequencing demonstrates the molecular and cellular reprogramming of metastatic lung adenocarcinoma. Nat Commun 11, 2285 (2020).
57. Kaslovsky, RA, Purdy, S, Dangman, BC, McKenna, BJ, Brien, T & Lives, R. Bronchioloalveolar Carcinoma in a Child With Congenital Cystic Adenomatoid Malformation*. CHEST 112, 548–551 (1997).
58. Benjamin, DR & Cahill, JL. Bronchioloalveolar carcinoma of the lung and congenital cystic adenomatoid malformation. Am J Clin Pathol 95, 889–892 (1991).
59. Ioachimescu, OC & Mehta, AC. From cystic pulmonary airway malformation, to bronchioloalveolar carcinoma and adenocarcinoma of the lung. Eur Respir J 26, 1181–1187 (2005).
60. Ramos, SG, Barbosa, GH, Tavora, FR, Jeudy, J, Torres, LAGM, Tone, LG et al. Bronchioloalveolar carcinoma arising in a congenital pulmonary airway malformation in a child: case report with an update of this association. Journal of Pediatric Surgery 42, e1–e4 (2007).
61. Summers, RJ, Shehata, BM, Bleacher, JC, Stockwell, C & Rapkin, L. Mucinous adenocarcinoma of the lung in association with congenital pulmonary airway malformation. J Pediatr Surg 45, 2256–2259 (2010).
62. Dosanjh, A. Bronchioalveolar carcinoma in a 15-year-old girl. Clin Pediatr (Phila) 31, 253–254 (1992).
63. Ohye, RG, Cohen, DM, Caldwell, S & Qualman, SJ. Pediatric bronchioloalveolar carcinoma: a favorable pediatric malignancy? J Pediatr Surg 33, 730–732 (1998).
64. Tassi, V, Daddi, N, Altimari, A, Gruppioni, E, Crinò, L, Rossi, G et al. Sarcomatoid change in adenocarcinoma arising in adulthood congenital pulmonary airway malformation. Adv Respir Med (2022) https://doi.org/10.5603/ARM.a2022.0008.
65. Mitchell, BJ, Rogers, GF & Wood, BC. A Patient With Schimmelpenning Syndrome and Mosaic KRAS Mutation. Journal of Craniofacial Surgery 30, 184–185 (2019).
66. Lihua, J, Feng, G, Shanshan, M, Jialu, X & Kewen, J. Somatic KRAS mutation in an infant with linear nevus sebaceous syndrome associated with lymphatic malformations. Medicine (Baltimore) 96, e8016 (2017).
67. Wang, H, Qian, Y, Wu, B, Zhang, P & Zhou, W. KRAS G12D mosaic mutation in a Chinese linear nevus sebaceous syndrome infant. BMC Medical Genetics 16, 101 (2015).
68. Slack, JC, Bründler, M-A, Chang, CA, Perrier, R, Lafay-Cousin, L & Kurek, KC. Bilateral Nephroblastic Tumors and a Complex Renal Vascular Anomaly in a

Patient With a Mosaic RASopathy: Novel Histopathologic Features and Molecular Insights. Pediatr Dev Pathol 24, 235–240 (2021).
69. Guo, H, Cajaiba, MM, Borys, D, Gutierrez, MC, Yee, H, Drut, RM et al. Expression of epidermal growth factor receptor, but not K-RAS mutations, is present in congenital cystic airway malformation/congenital pulmonary airway malformation. Hum Pathol 38, 1772–1778 (2007).
70. de Cordova, XF, Wang, H, Mehrad, M, Eisenberg, R, Johnson, J, Wei, Q et al. Mucinous Adenocarcinoma With Intrapulmonary Metastasis Harboring KRAS and GNAS Mutations Arising in Congenital Pulmonary Airway Malformation. Am J Clin Pathol 156, 313–319 (2021).
71. Koopman, T, Rottier, BL, Ter Elst, A & Timens, W. A case report of an unusual non-mucinous papillary variant of CPAM type 1 with KRAS mutations. BMC Pulm Med 20, 52 (2020).

ACKNOWLEDGEMENTS

This project was funded by the Society for Pediatric Pathology Young Investigator Grant (J.P.) and the Doris Duke Charitable Foundation Clinical Scientist Development award and Ayla Gunner Prushansky Research Fund (DBF) and the NIH (K08 HL140129) (DBF). Portions of this work were presented at the annual meetings for the Society for Pediatric Pathology (March 2020 and 2021) and USCAP (March 2022).

AUTHOR CONTRIBUTIONS

J.P. conceptualized the study, and J.P., N.D.N., M.L., D.B.F., and W.H.P. planned the study design. N.D.N., J.P., F.X., M.L., P.C., and D.B.F. provided acquisition, analysis and interpretation of data, and developed methodology. L.A.L. selected and reviewed adult adenocarcinomas included in the study. N.D.N. performed statistical analysis. The initial manuscript was written by N.D.N. and J.P., and all authors participated in subsequent review and revision. All authors approved the final paper.

COMPETING INTERESTS

The authors declare no competing interests.

ETHICS APPROVAL

This study was approved by the institutional review boards of the Children's Hospital of Philadelphia (20-017451) and Hospital of the University of Pennsylvania (843704).

ADDITIONAL INFORMATION

Supplementary information The online version contains supplementary material available at https://doi.org/10.1038/s41379-022-01129-0.

Correspondence and requests for materials should be addressed to Jennifer Pogoriler.

Reprints and permission information is available at http://www.nature.com/reprints

Publisher's note Springer Nature remains neutral with regard to jurisdictional claims in published maps and institutional affiliations.